

MAEG 5725 Homework Design Problem 1

Teaching Assistant: LIU Kangcheng

1 Problem Overview and background

In this design problem, we need to design the controller for an unmanned helicopter flight control system. The modelling part of the Helion has been completed and the state space representation has been given. What is required is that we should use the LQR controller design, the Kalman filter and their combination, the LQG/LQR control methodology to design a measurement feedback control law that meet the following specifications:

1. The overall system is stabilized;
2. The dynamics of the helicopter will be driven to the hovering state, i.e. all state variables are to be driven to 0, as quickly as possible from the given initial condition.

The proposed LQG/LQR controller design has been developed by researchers is mature and well-established. Without concerning about the derivation of the controller, we can design the controller by just following 3 simple steps given in the lecture notes prepared by Professor Ben M. Chen.

2 Model of HeLion

According to the given parameters, the unmanned aerial vehicle (UAV) platform HeLion has a linearized state space model which is described as:

$$\begin{aligned}\dot{x} &= Ax + Bu \\ y &= Cx\end{aligned}\tag{1}$$

where

$$A = \begin{bmatrix} 0 & 0 & 1 & 0 & 0 & 0 & 0.0009 & 0 & 0 \\ 0 & 0 & 0 & 0.992 & 0 & 0 & -0.0389 & 0 & 0 \\ 0 & 0 & -0.0302 & -0.0056 & -0.0003 & 585.1165 & 11.4448 & -59.529 & 0 \\ 0 & 0 & 0 & -0.0707 & 267.7499 & -0.0003 & 0 & 0 & 0 \\ 0 & 0 & 0 & -1 & -3.3607 & 2.2223 & 0 & 0 & 0 \\ 0 & 0 & -1 & 0 & 2.4483 & -3.3607 & 0 & 0 & 0 \\ 0 & 0 & 0.0579 & 0.0108 & 0.0049 & 0.0037 & -21.9557 & 114.2 & 0 \\ 0 & 0 & 0 & 0 & 0 & 0 & -1 & 0 & 0 \\ 0 & 0 & 0 & 0.389 & 0 & 0 & 0.992 & 0 & 0 \end{bmatrix}$$

$$B = \begin{bmatrix} 0 & 0 & 0 \\ 0 & 0 & 0 \\ 0 & 0 & 43.3635 \\ 0 & 0 & 0 \\ 0.2026 & 2.5878 & 0 \\ 2.5878 & -0.0663 & 0 \\ 0 & 0 & -83.1883 \\ 0 & 0 & -3.8500 \\ 0 & 0 & 0 \end{bmatrix}, C = \begin{bmatrix} 1 & 0 & 0 & 0 & 0 & 0 & 0 & 0 & 0 \\ 0 & 1 & 0 & 0 & 0 & 0 & 0 & 0 & 0 \\ 0 & 0 & 1 & 0 & 0 & 0 & 0 & 0 & 0 \\ 0 & 0 & 0 & 1 & 0 & 0 & 0 & 0 & 0 \\ 0 & 0 & 0 & 0 & 0 & 0 & 1 & 0 & 0 \\ 0 & 0 & 0 & 0 & 0 & 0 & 0 & 1 & 0 \\ 0 & 0 & 0 & 0 & 0 & 0 & 0 & 0 & 1 \end{bmatrix}$$

In addition, in the second part of the simulation, a disturbance of wind gust disturbance will be considered in the problem formulation. Therefore the dynamical equation can be modified as:

$$\begin{aligned} \dot{x} &= Ax + Bu + Ew \\ y &= Cx \end{aligned} \quad (2)$$

where

And the problem formulation can be further considered as

$$\begin{aligned} \dot{x} &= Ax + [B \quad E] \begin{bmatrix} u \\ w \end{bmatrix} \\ y &= Cx \end{aligned} \quad (3)$$

which will facilitate the simulation and make it easier for us to take all the disturbance into consideration.

3 The LQG/LQR Controller Design

The initial condition in our simulation is

$$x_0 = \begin{bmatrix} 0 \\ -0.1 \\ 0 \\ 0 \\ 0 \\ 0 \\ 0 \\ 0 \\ 0.1 \end{bmatrix}$$

Physically, it means the helicopter is commanded to hover from a pitch angle of -0.1 rad (a nose-down angle of 5.7 degrees) and yaw angle of 0.1 rad (5.7 degrees). Other design considerations, such as frequency domain requirements on gain and phase margins, are to be ignored. and due to physical limitation, they will have to be kept within the following limits:

$$|\delta_{lat}| < 0.35 \quad |\delta_{lon}| < 0.35 \quad |\delta_{ped}| < 0.4$$

In order to design a LQG control law for this system, 3 major steps to fulfill the requirements are as shown below.

3.1 LQR Control Law

As is mentioned above, the system is characterized by In the first step, we will design an LQR controller with control law $u = -Fx$ which minimize the energy function

$$J = \int_0^\infty (x^T Q x + u^T R u) dt, \quad Q \geq 0, R > 0$$

with the system $\dot{x} = Ax + Bu$ by solving the Ricatti Equation:

$$PA + A^T P - PBR^{-1}B^T P + Q = 0, P > 0$$

and the controller gain, $F = R^{-1}B^T P$. It can be easily solved by using Matlab function `[K, S, e] = lqr(A,B,Q,R)`. In our case, if we select both the matrix Q and R to be identity matrices, we can easily obtain the feedback gain as follows:

$$F = \begin{bmatrix} 0.9426 & 0.0345 & 0.6518 & 0.0389 & 1.2531 & 15.9737 & 0.3559 & -0.0816 & 0.3321 \\ -0.0464 & 0.9985 & 0.0250 & 0.7241 & 11.0125 & -0.0183 & -0.0121 & 0.0027 & 0.0280 \\ 0.3306 & 0.0418 & 0.3536 & 0.0041 & -0.0445 & -0.3946 & -0.7216 & -1.9072 & -0.9428 \end{bmatrix}$$

We can also check that the closed-loop system is stable by evaluating the closed-loop poles with the help of Matlab. Here, the poles are all located in the open left half plane as shown below.

$$-93.6476 + 0.0000i$$

$$\begin{aligned}
& -22.6826 + 30.8785i \\
& -22.6826 - 30.8785i \\
& -15.6238 + 22.3602i \\
& -15.6238 - 22.3602i \\
& -5.3713 + 0.0000i \\
& -0.9245 + 0.0000i \\
& -0.9338 + 0.0000i \\
& -0.9674 + 0.0000i
\end{aligned}$$

3.2 The Kalman filter Design

Due to measurement noise and the existence of unmeasurable state variables, an observer is needed to observe the system's states. In this second step, we are required to design a Kalman filter for the plant to estimate the state variables of the system. Similar to the previous problem, Kalman filter can be designed by choosing an appropriate Q_e and R_e matrix and solving the Riccati Equation

$$P_e A + A^T P_e - P_e B R_e^{-1} C P_e + Q_e = 0, P_e > 0$$

and the Kalman gain, $K_e = P_e C^T R^{-1}$. Similarly, it can also be solved easily by utilizing the Matlab function $[L, P, e] = \text{lqe}(Ae, Ge, Ce, Qe, Re)$. In my design, both Q_e and R_e are chosen as identity matrices, and the resulting designed P_e matrix in Kalman filter is given as follows:

$$P_e = \begin{bmatrix} 1.2349 & 0.0021826 & 0.31175 & 0.036871 & -0.0022967 & -0.021934 & -0.0049735 & -0.0016775 & 0.00072337 \\ 0.0021826 & 1.2337 & -0.028786 & 0.31239 & -0.028769 & -0.0028283 & -0.0085133 & -0.0013292 & 0.0012958 \\ 0.31175 & -0.028786 & 19.243 & 1.6 & 0.12338 & 0.31616 & 0.067759 & -0.013504 & 0.006062 \\ 0.036871 & 0.31239 & 1.6 & 11.867 & 0.26921 & 0.029023 & 0.02094 & 0.0041945 & 0.010618 \\ -0.0022967 & -0.028769 & 0.12338 & 0.26921 & 0.060166 & 0.0070558 & 0.00059858 & 0.00021664 & -0.0012229 \\ -0.021934 & -0.0028283 & 0.31616 & 0.029023 & 0.0070558 & 0.044767 & 0.0072719 & 0.0023516 & -0.0010406 \\ -0.0049735 & -0.0085133 & 0.067759 & 0.02094 & 0.00059858 & 0.0072719 & 0.4136 & 0.25916 & 0.039111 \\ -0.0016775 & -0.0013292 & -0.013504 & 0.0041945 & 0.00021664 & 0.0023516 & 0.4136 & 0.10529 & 0.039111 \\ 0.00072337 & 0.0012958 & 0.006062 & 0.010618 & -0.0012229 & -0.0010406 & 0.25916 & 0.039111 & 1.2047 \end{bmatrix}$$

$$F = \begin{bmatrix} 1.2349 & 0.0022 & 0.3117 & 0.0369 & -0.0050 & 0.0007 \\ 0.0022 & 1.2337 & -0.0288 & 0.3124 & -0.0085 & 0.0013 \\ 0.3117 & -0.0288 & 19.2430 & 1.6000 & 0.0678 & 0.0061 \\ 0.0369 & 0.3124 & 1.6000 & 11.8670 & 0.0209 & 0.0106 \\ -0.0023 & -0.0288 & 0.1234 & 0.2692 & 0.0006 & -0.0012 \\ -0.0219 & -0.0028 & 0.3162 & 0.0290 & 0.0073 & -0.0010 \\ -0.0050 & -0.0085 & 0.0678 & 0.0209 & 2.0746 & 0.2592 \\ -0.0017 & -0.0013 & -0.0135 & 0.0042 & 0.4136 & 0.0391 \\ 0.0007 & 0.0013 & 0.0061 & 0.0106 & 0.2592 & 1.2047 \end{bmatrix}$$

We can verify that the designed observer is stable by evaluating the observer pole positions. Here all the poles are at open left half plane as shown below.

$$\begin{aligned}
& -11.2528 + 26.4828i \\
& -11.2528 - 26.4828i \\
& -7.7369 + 17.8813i \\
& -7.7369 - 17.8813i
\end{aligned}$$

$$\begin{aligned}
& -11.9919 + 4.1354i \\
& -11.9919 - 4.1354i \\
& -1.2207 + 0.0000i \\
& -1.2242 + 0.0000i \\
& -1.2277 + 0.0000i
\end{aligned}$$

3.3 LQG Control Law

In the last step, the LQG control law can be adopted by assigning $u = -F \hat{x}$, in which \hat{x} is the output of the Kalman filter from the previous step, and u is the input to the UAV plant. We can get the LQG control law by just combine the LQR and kalman filter.

$$\begin{aligned}
\dot{\hat{x}} &= (A - BF - K_e C) \hat{x} + K_e y \\
u &= -F \hat{x}
\end{aligned} \tag{4}$$

We can show the relationship in Fig. 1.

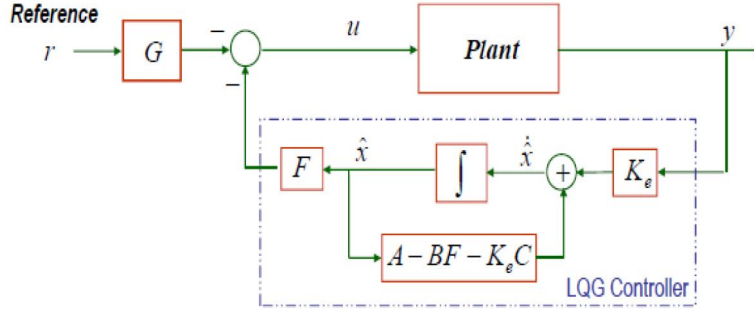


Figure 1: The LQG controller

4 Simulation Results

Since the UAV model parameters and controller gains have been already derived in the previous section, simulation can be done by using Matlab and Simulink. In this section, two simulation results will be provided:

1. closed-loop system with input and measurement noise;
2. closed-loop system with input and measurement noise, together with a wind gust disturbance in the form of sine wave to the velocity channels.

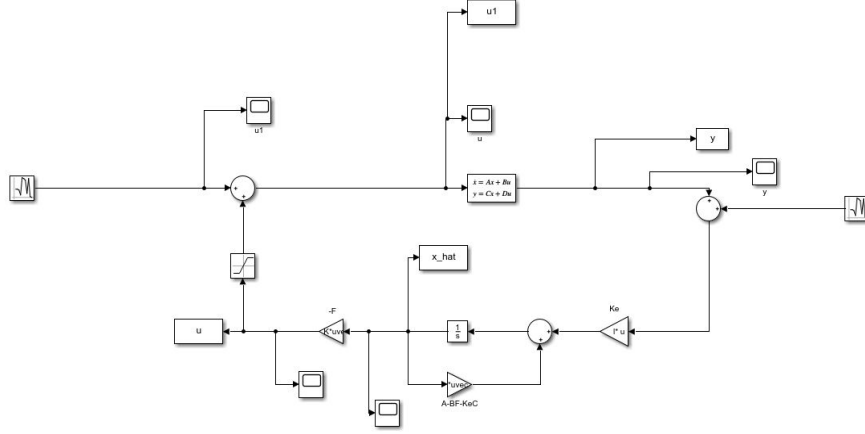


Figure 2: Simulink block diagram of LQG design

4.1 With Input and Measurement Noise

Fig. 2 shows the Simulink block diagram of the controller design in this part. Here, the random noise added to the input and the measurement output are in normal distribution with mean 0 and variance 0.01. In this simulation, both Q and R of the LQR controller is set to be identity matrix, while both Q_e and R_e of the Kalman filter are also set as identity matrix. The simulation results in Fig. 3 to Fig. 5 has verified that this set of matrices is able to give good responses to the closed-loop system. Specifically, Fig. 3 shows the $\phi, \theta, \psi, p, q, r$ of the UAV in simulation from time $t = 0$ to $t = 10$ sec. For all the 6 state variables, Kalman filter not only is able to track the measurement output, but eliminate portion of the noise to give us a smooth response. Also noted that all the 6 state variables converges to 0 (hovering flight) after a short period within 5 seconds. Particularly, we remember that the initial condition of the pitch angle θ is given as -0.1 m/s, while the initial condition for the Kalman filter is set as 0. Thus base on the result in the pitch angle channel, it shows that the designed observer is able to trace the real output even if there is an error in the initial response.

One might notice that there is a little positive overshoot of the angular rate q during the initial response. It indicates that there is a positive rotation movement on the pitch angle of the UAV, which possibly caused by the movement of the swashplate of HeLion, as a result to break its momentum from moving forward. It can be seen as an effort of braking to stop the UAV from moving forward, which makes good sense of what this controller is trying to achieve: to reach hover state from forward-moving state.

Fig. 4 shows the estimation of the immeasurable internal dynamic state variables $a_s; b_s; \delta_{ped,int}$. Here, we can not obtain the measurement of these 3 state

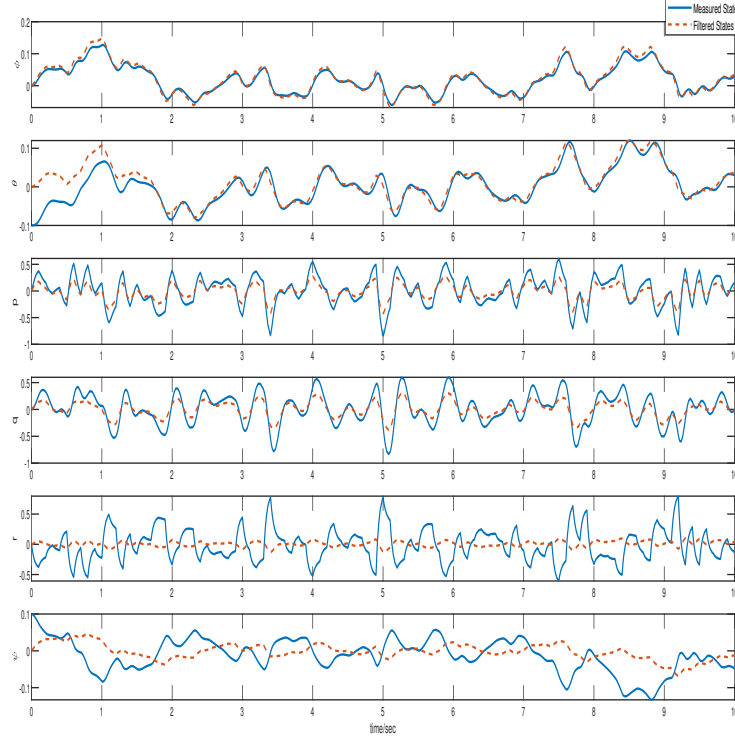


Figure 3: States of the UAV

variables, and hence only estimations are given. Similar to the response above, the state variables converges to 0 after a short period. Again, judging from the plot of θ , it justifies the discussion mentioned in the last paragraph. Lastly, Fig. 5 shows the control input to the UAV. All the control inputs are reasonable within the limit given. It concludes that the controller works well even under minor input and measurement noise.

4.2 With Input and Measurement Noise and wind gust disturbance

Fig. 6 shows the Simulink block diagram of the controller design in this part. Take note that the random noise added to the input and the measurement output are similar to the previous part. The additional disturbances added to

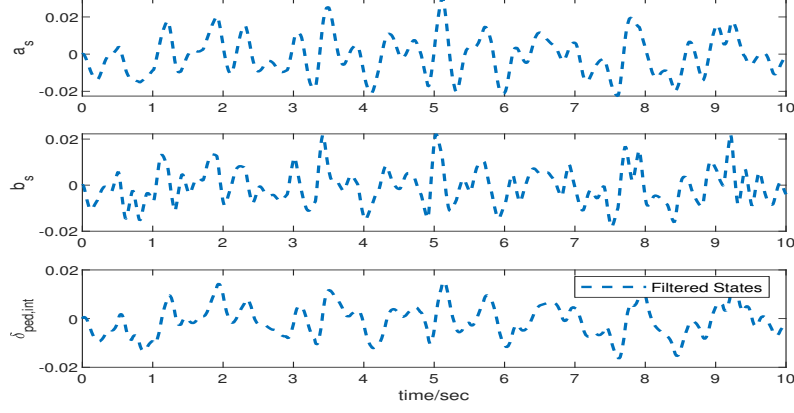


Figure 4: The immeasurable filtered States of the UAV

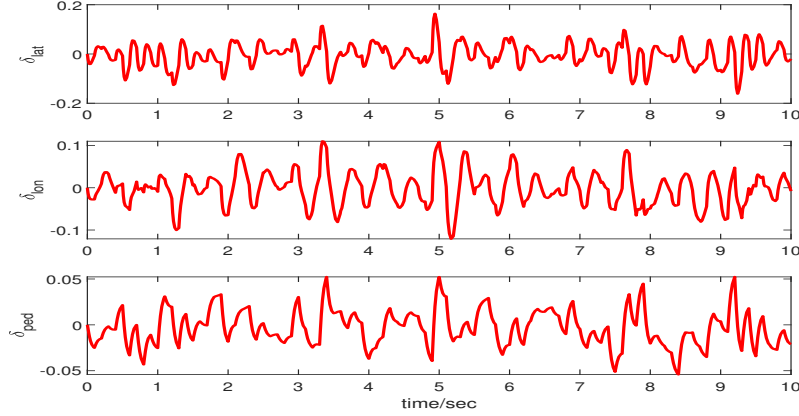


Figure 5: Control Inputs of UAV

the system is in the form of

$$\begin{pmatrix} U_{wind} \\ V_{wind} \\ W_{wind} \end{pmatrix} = \begin{pmatrix} 10\cos(\frac{2\pi}{40}(t-20)) \\ 10\cos(\frac{2\pi}{40}(t-20)) \\ 3\cos(\frac{2\pi}{40}(t-20)) \end{pmatrix}, 10 \leq t \leq 30$$

to the translational velocities of the system, i.e. $U; V; W$. The disturbances block is inserted to the simulation block diagram shown in Fig 6.

Fig. 7 shows the $\phi, \theta, \psi, p, q, r$ of the UAV in simulation from time $t = 0$ to $t = 40$ secs in detail. However, at time $t = 10$ to $t = 30$ sec, the UAV is undergoing wind gust disturbances. The simulation results show that the controller is able to resist the disturbance well, all state variables will converge to zero and the

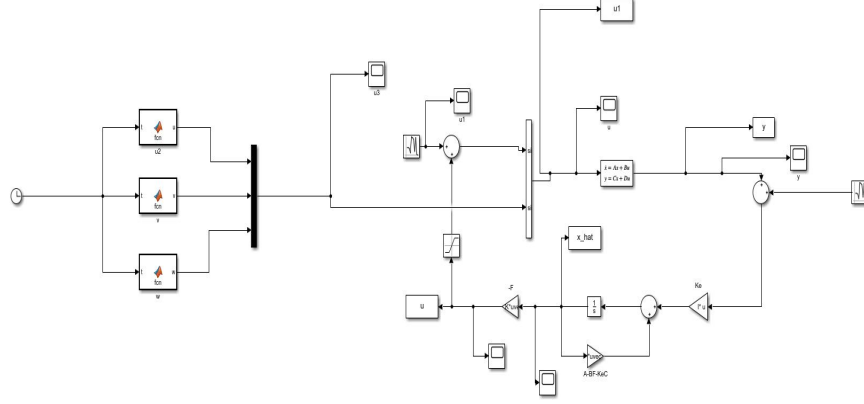


Figure 6: Simulink block diagram of LQG design with wind gust disturbance

disturbance will be rejected effectively.

Fig. 8 shows the estimation of the immeasurable internal dynamic state variables a_s ; b_s ; $\delta_{ped,int}$. Here, we can not obtain the measurement of these 3 state variables, and hence only estimations are given. Similar to the response above, the state variables nearly converges to 0 after a short period. But we can still see that the the LQG control law is not very robust under large wind gust disturbance.

Lastly, Fig. 9 shows the control inputs to the UAV. All the control inputs are reasonable within the limit given.

For both the simulation, one might observe that by relaxing the weight on the control input gain (increase Q matrix or decrease R matrix) will improve the performance of the UAV with or without wind gust disturbances. However, due to the limitation in the control input, the modification will cause large control input and hence violate the given specification. This poses a typical trade-off scenario where good control performance and low control effort has to be chosen depends on the application needs.

5 Conclusion

In conclusion, as can be seen from the results, the LQG/LQR controller is good at estimating states with input and measurement noises. However, it is weaker to reject disturbances, such as the wind gust disturbances shown in this assignment. The disturbance rejection performance is not very robust. Therefore we need a more robust controller that has a capability to decrease the effect of the disturbances, such as H_2 and H_∞ controller.

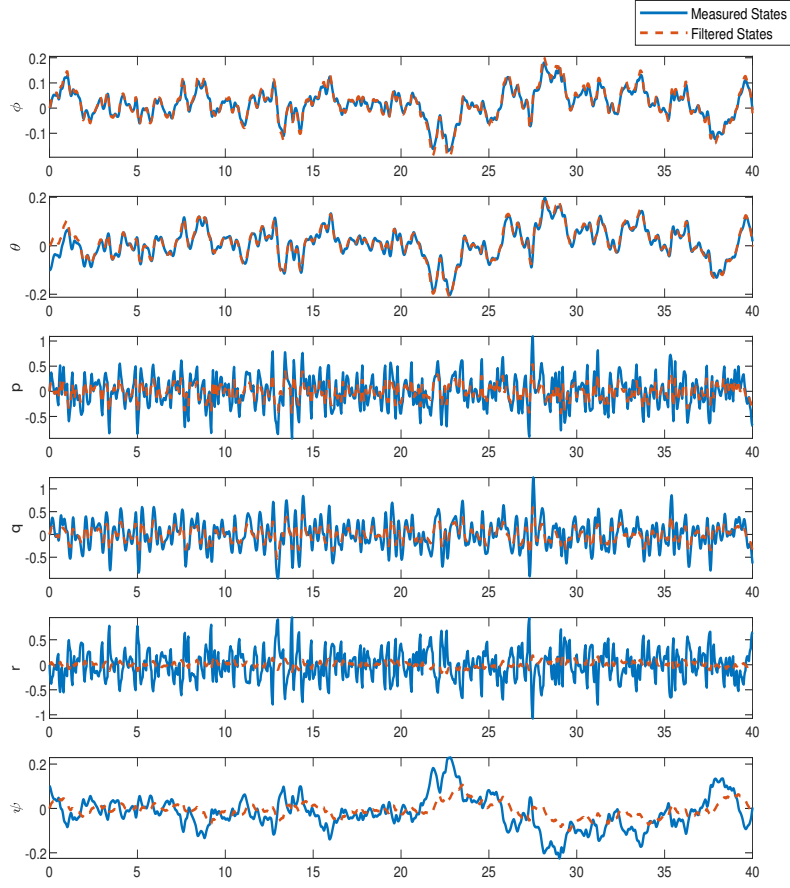


Figure 7: States of UAV with wind gust disturbance

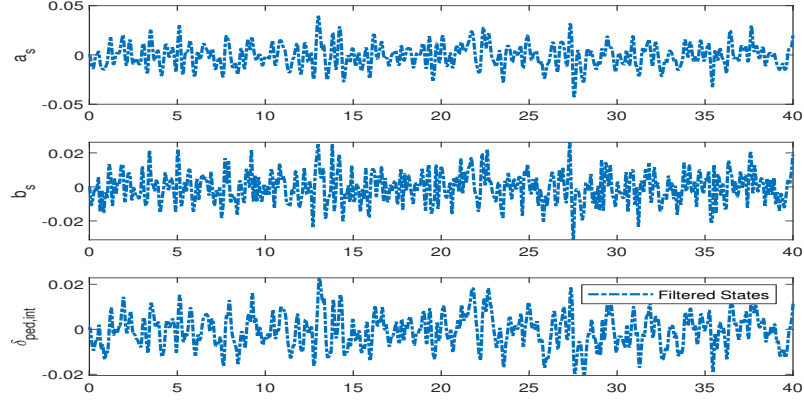


Figure 8: Immeasurable States of UAV with wind gust disturbance

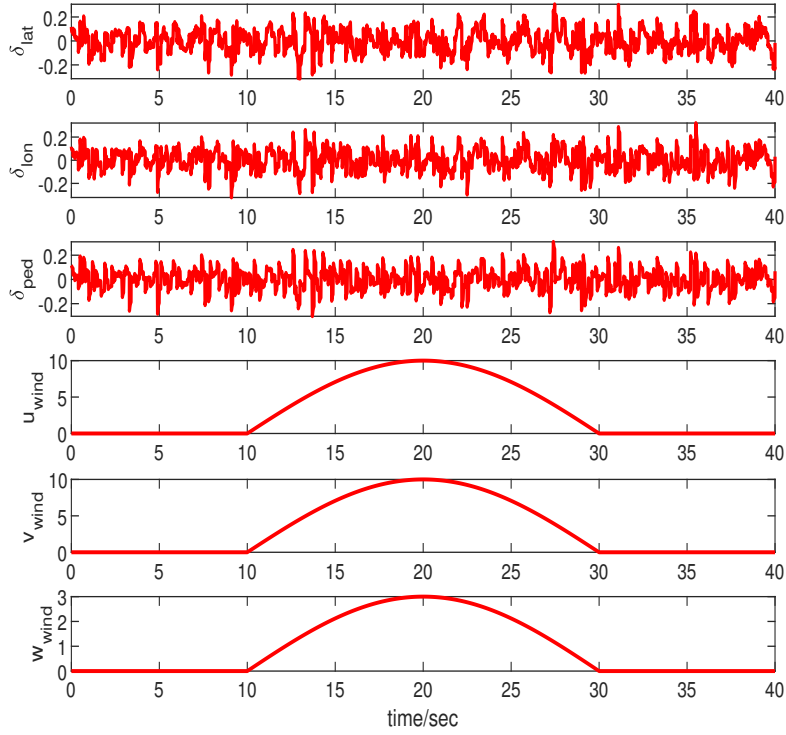


Figure 9: Control and disturbance inputs of LQG design with wind gust disturbance